Physicochemical study of bulk Dy-123 doped with nano-Fe_3O_4

A. Stoyanova-Ivanova[1], S. Kolev[2,3*], V. Petrova[1], O. Petkov[1], L. M. Tran[4], M. Babij[4], A. Zaleski[4], V. Mikli[5], D. Kovacheva[6]

[1] G. Nadjakov Institute of Solid State Physics, Bulgarian Academy of Sciences, 72 Tsarigradsko Chaussee, 1784 Sofia, Bulgaria

[2]Institute of Electronics, Bulgarian Academy of Sciences, 72 Tsarigradsko Chaussee, 1784 Sofia, Bulgaria
[3]Neofit Rilski South-Western University, 66 Ivan Mihailov Str., 2700 Blagoevgrad, Bulgaria
[4] Institute of Low Temperature and Structure Research, Polish Academy of Sciences, ul. Okolna 2, 50-422 Wroclaw, Poland

[5] Institute of Materials and Environmental Technology, Tallinn University of Technology, 19086 Tallinn, Estonia
[6] Institute of General and Inorganic Chemistry, Bulgarian Academy of Sciences, G. Bonchev Str., bl.11, 1113 Sofia, Bulgaria

$DyBa_2Cu_3O_{7-\beta}$, or Dy-123, is a superconducting material with a high T_c. We synthesized a bulk ceramic Dy123 composite by a solid-state reaction with a starting stoichiometry of 1:2:3 (Dy:Ba:Cu). The reagents were Dy_2O_3, $BaCO_3$ and CuO with analytical grade purity and were mixed by grinding in an agate mortar. The resulting mixture was calcined at 900 ºC in a flowing oxygen atmosphere for 21 h. The calcined powder was reground and sintered again at 940 ºC for 21 h with additional annealing at 450 ºC in an oxygen atmosphere for 2 h. Further, the obtained powder was reground, mixed with 2 wt. % of Fe_3O_4 nanopowder, homogenized and then pressed into tablets at 4 MPa. The bulk sample was sintered at 930 ºC in a flowing oxygen atmosphere for 24 h and annealed at 450 ºC in an oxygen atmosphere for 4 h. The phase composition, the microstructure and the superconducting properties of the sample were investigated.

Keywords: superconductors, nanoparticles, magnetite

INTRODUCTION

$ReBa_2Cu_3O_{7-\beta}$ or Re-123 (Re = rare earth element, such as Y, Eu, Gd, Dy, Nd, Sm, Ho, Er) materials are known as being superconductors with a high T_c [1]. Their properties are suitable for high-field electronic applications, such as magnetic bearings, permanent magnets, power cables, etc. Different theoretical models have been used to explain the varying T_c and the transition superconductor-insulator properties of the compound – hole filling [2], hole localization in the CuO_2 plane [3, 4], oxygen deficiency in the CuO chains leading to orthorhombic-tetragonal phase transition at its critical temperature. The higher the oxygen content, the lower the T_c [5].

The crystal structure of the ReBCO-based compounds is a multilayered perovskite structure. The layers are separated by two different Cu-sites: Cu(1) site in CuO chains and Cu(2) site in CuO_2 planes. The planes are believed to be the reason for the superconductive properties of the compound, while the chains are non-superconductive charge reservoirs introducing holes into the CuO_2 planes [6-8].

The studies carried out so far have shown that Re-123 exhibit better properties (higher transition temperatures, better performance in external magnetic fields, better surface morphology) and are more easily applicable compared to the Y123 system [9-12]. Boonsong *et al.* synthesized DyBCO ceramics under different temperatures and analyzed them, finding that the $DyBa_2Cu_3O_{7-\beta}$ (Dy123) phase was the main crystalline phase in all samples. An oxygen stoichiometric change has also been observed that seems to largely affect the structural transformation of the material system [13]. On the other hand, another way of influencing the properties of the HTSC ReBCO ceramics is introducing dopants during the ceramic processing. Among the different elements studied as dopants have been Ca, K [14, 15], Ag [16] and Fe [17]. Adding ferrite nanoparticles has been reported to further improve the morphology and the magnetic flux pinning [18]. Abd-Ghani *et al.* studied the influence of Fe_3O_4 magnetic nanoparticles on the properties of YBCO superconductors and proposed that a small amount of this additive acts as effective flux pinning centers and can be applied in order to improve the critical transport current density of the

---

superconductor [17].

The aim of this study is, therefore, to synthesize and characterize DyBCO ceramic with a nano-Fe_3O_4 additive in terms of identifying the phase and elemental composition, the microstructure and the superconducting transition temperature and follow any changes in the material's properties.

Experimental procedure

A bulk ceramic composite Dy123 was synthesized by a solid-state reaction with a starting stoichiometry of 1:2:3 (Dy:Ba:Cu). The reagents were Dy_2O_3, $BaCO_3$ and CuO with analytical grade purity mixed by grinding in an agate mortar. The resulting mixture was calcined at 900 °C in a flowing oxygen atmosphere for 21 h. The calcined powder was reground and sintered again at 940 °C for 21 h with additional annealing at 450 °C in an oxygen atmosphere for 2 h. Further, the obtained powder was reground, mixed with 2 wt.% of Fe_3O_4 nanopowder obtained by the microemulsion technique [19], homogenized and then pressed into tablets at 4 MPa. The bulk sample was sintered at 930 °C in a flowing oxygen atmosphere for 24 h and annealed at 450 °C in an oxygen atmosphere for 4 h.

Experimental methods

The X-ray diffraction patterns of the superconducting powder sample were obtained within the range 5.3 – 80°2θ at a constant step of 0.02°2θ on a Bruker D8 Advance diffractometer with Cu Kα radiation and a LynxEye detector. The phase identification was performed by the Diffracplus EVA program using the ICDD-PDF2 (2014) database. The mean crystallite size was determined by the Topas-4.2 software package using the fundamental parameters peak-shape description including appropriate corrections for the instrumental broadening and diffractometer geometry.

The microstructure of the samples was studied by means of a Zeiss EVO MA-15 scanning electron microscope (SEM) with a LaB6 cathode on the polished cross-section of the samples. The chemical composition was determined by X-ray microanalysis using energy dispersive spectroscopy (EDS) on an Oxford Instruments INCA Energy system. The qualitative and quantitative analyses were carried out at an accelerating voltage of 20 kV.

RESULTS AND DISCUSSION

Fig. 1 shows the XRD patterns of pure Dy123 and Dy123+Fe_3O_4 samples. The high-intensity peaks are assigned to the respective samples. The XRD analysis was conducted on the whole sample surface and did not detect phases with an amount under 4%. Adding such a small amount of Fe_3O_4 nanoparticles does not affect the cell parameters, as the Fe_3O_4 does not enter the DyBCO crystal structure. For the same reason, no peaks are detected assigned to pure nano Fe_3O_4 in the XRD patterns.

The XRD analysis showed that the pure Dy123 and the Dy123 with Fe_3O_4 have the same $DyBa_2Cu_3O_7$ phase with orthorhombic structure and lattice parameters $a = 3.887$ Å, $b = 3.825$ Å and $c = 11.686$ Å, as well as the same cell volume (V) of 173.745 Å³. The addition of 2 wt. % of nano-Fe_3O_4 to the ceramic sample does not affect the cell lattice parameters. The results thus obtained for the lattice parameters of pure Dy123 correspond to the ones obtained by other authors [13].

To calculate the oxygen content in the investigated HTSC ceramics, we used an equation establishing a correlation between the c lattice parameter and the oxygen coefficient (y) in the $ReBa_2Cu_3O_y$ ceramic [21]. The results quoted in Table 2 show that the oxygen content in the sample with Fe_3O_4 is the same as in the pure one. We, therefore, assume that adding 2 wt.% of Fe_3O_4 nanopowder to the DyBCO ceramic investigated did not influence the amount of oxygen, the latter being important for its superconducting properties.

Table 1. Lattice parameters of pure Dy123 and Dy123 + Fe_3O_4 samples obtained by XRD analysis

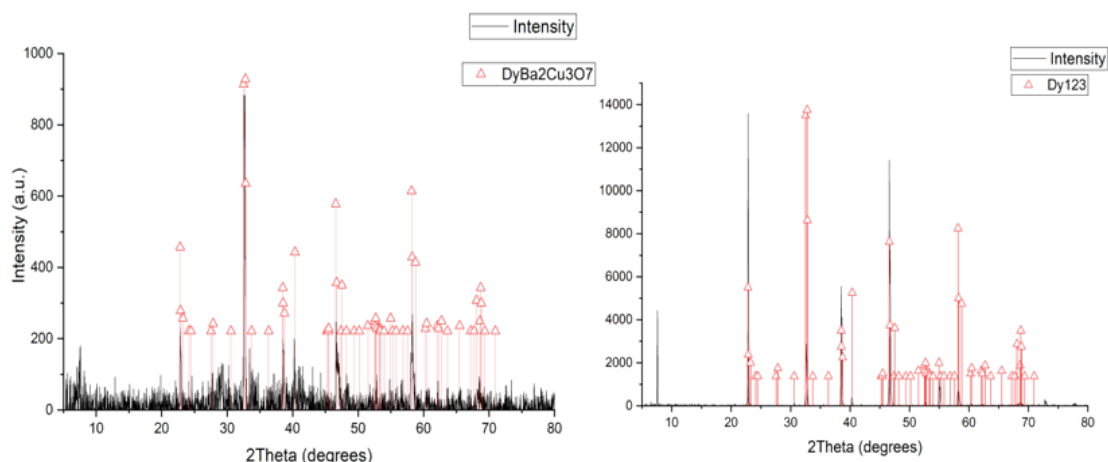| Phase	Type	Lattice parameter			V
		a [Å]	b [Å]	c [Å]	[Å³]
Sample		Dy123			
$DyBa_2Cu_3O_7$	Orthorhombic	3.887	3.825	11.686	173.745
Sample		Dy123 + Fe_3O_4			
$DyBa_2Cu_3O_7$	Orthorhombic	3.887	3.825	11.686	173.745
Sample		Dy123 [20]			
$DyBa_2Cu_3O_7$	Orthorhombic	3.839	3.889	11.687	174.485

Fig. 1. XRD patterns of pure Dy123 (left) and Dy123 synthesized + Fe₃O₄ (right)

Table 2. Calculation of the oxygen content in the samples studied

Sample	Lattice parameter c [Å]	Equation $y = f(c)$	Calculated oxygen
Dy23	11.686	$y = 74.843 - 5.814\ c$	6.901
Dy123 + Fe₃O₄	11.686		6.901

Table 3. Elemental composition of the Dy123 + Fe₃O₄ sample obtained by EDX analysis

Spectrum / Element	Series	1 Atom. C. [at. %]	2 Atom. C. [at. %]	3 Atom. C. [at. %]	4 Atom. C. [at. %]	5 Atom. C. [at. %]	6 Atom. C. [at. %]
Dysprosium	L	11.65	0.28	0	4.68	4.71	4.30
Barium	L	9.04	0.26	12.59	9.34	9.39	8.52
Copper	K	11.13	44.99	17.70	13.25	13.22	14.61
Oxygen	K	68.19	54.47	57.07	71.57	71.40	71.13
Chlorine	K	0	0	12.33	0	0	0.42
Iron	K	0	0	0.32	1.16	1.29	1.02
Phase		DyBaCu	CuO	BaCuO₂+ Fe	Dy123+ Fe	Dy123+ Fe	Dy123+ Fe

Fig. 2. SEM of Dy123 with Fe₃O₄

Fig. 2 shows a SEM micrograph of the sample Dy123 with Fe₃O₄ exhibiting a multiphase structure. The prevailing Dy123 phase has a typical surface with elongated grains and an average grain size of ~ 3.74 μm.

Table 3 summarizes the EDX results. They indicate that the ceramic has a non-monophasic composition. In the Dy123 with Fe₃O₄ sample, the Dy-123, BaCuO₂ and CuO phases are detected. The amount of Fe in the sample is found to be very small located around the main phases.

The EDX mapping analysis of the Dy123 with Fe₃O₄ sample (Fig. 3) confirms the presence of the main elements of the DyBCO ceramic, as well as the presence of Fe from the doping and small quantities of chlorine. We assume that the chlorine originates from the epoxy resin used to hold the sample during the test. Whole crystals of CuO and BaCuO₂ are visible on the surface, with small quantities of Fe also detected scattered around the Dy123, CuO and BaCuO₂ crystals. We believe that Fe does not react with the other elements and does not form phases of its own.
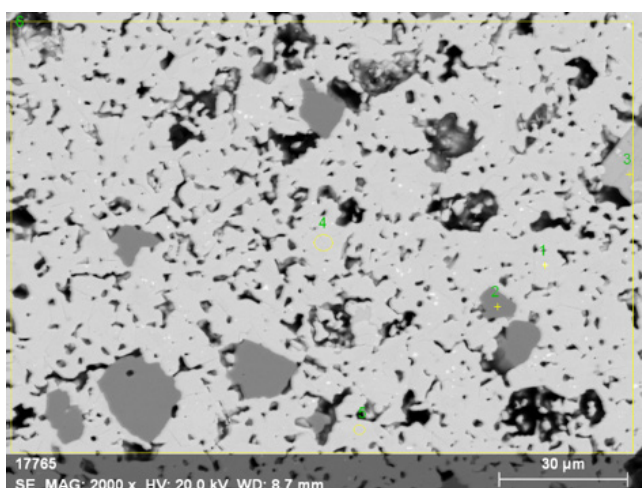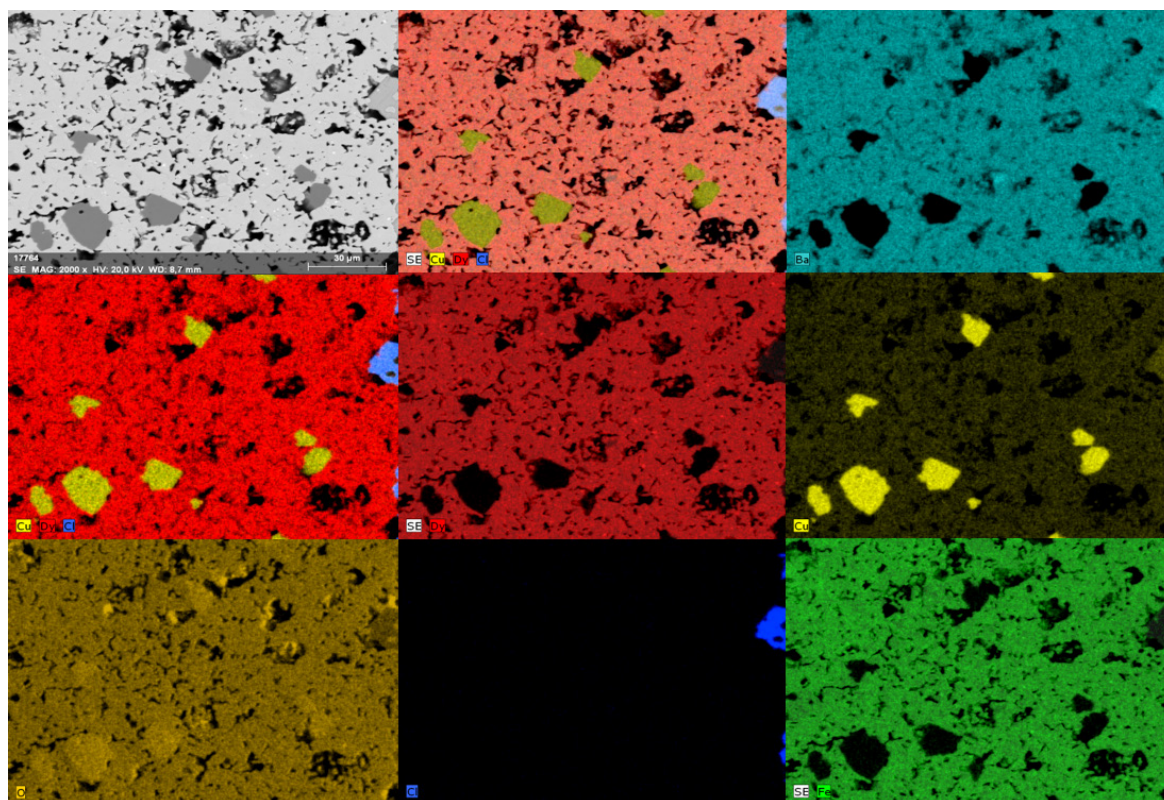
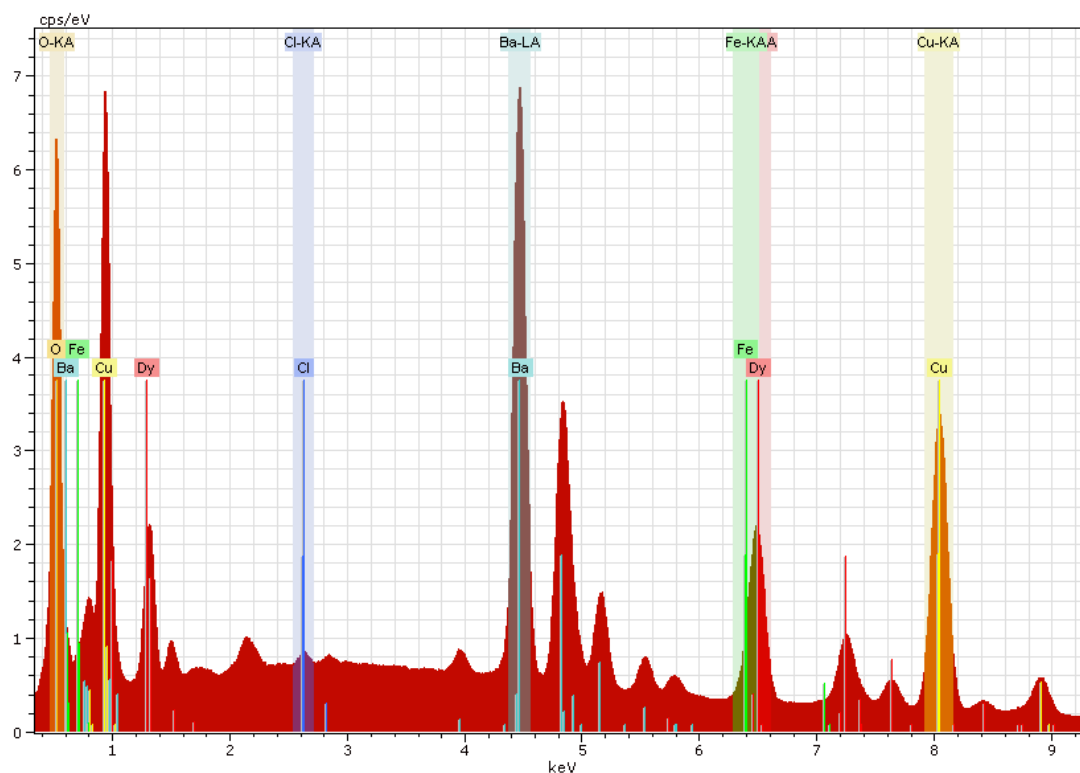**Fig. 3.** EDX mapping analysis of Dy123 with Fe$_3$O$_4$

Fig. 4. EDX spectra of the Dy123 sample with Fe$_3$O$_4$

The EDX spectra of the Dy123 sample with Fe$_3$O$_4$ (Fig. 4) exhibit lines for Dy (red), Ba (light green), Cu (yellow), O (dark yellow), Fe (green) and Cl (dark blue), which correspond to the literature table values for X-ray emission lines [25] of those elements. Respectively, $L_{\alpha1} = 6.50$ keV, $L_{\alpha2} = 6.46$ keV, $L_{\beta1} = 7.25$ keV, $L_{\beta2} = 7.64$ keV, $L_{\gamma1} = 8.42$ keV and $M_{\alpha1} = 1.29$ keV for Dy; $L_{\alpha1} = 4.47$ keV, $L_{\alpha2} = 4.45$ keV, $L_{\beta1} = 4.83$ keV, $L_{\beta2} = 5.16$ keV, $L_{\gamma1} = 5.53$ keV for Ba;

74

$K_{\alpha1} = 8.05$ keV, $K_{\alpha2} = 8.03$ keV, $K_{\beta1} = 8.91$ keV and L lines in the $0.92 – 0.95$ keV range for Cu; $K_{\alpha1} = 0.52$ keV for O and $K_{\alpha1} = 6.40$ keV, $K_{\alpha2} = 6.39$ keV, $K_{\beta1} = 7.06$ keV and L lines in the $0.70 – 0.72$ keV range for Fe. There are also spectral lines for Cl ($K_{\alpha1} = 2.62$ keV) detected in small quantities on the surface of the sample.
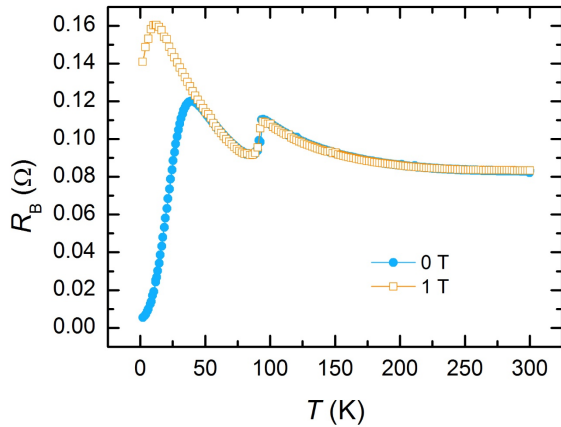
Fig 5. Electrical resistivity *versus* temperature for Dy123 with Fe_3O_4 without and with magnetic field of 1 T.

It has been found that barium cuprate is one of the few copper oxides exhibiting ferromagnetic interactions, so that during T_c measurements it can affect the transition width of the ρ-T curves. Studies have shown that, besides the superconducting properties, a composite ReBCO compound that contains $BaCuO_2$ exhibits magnetic properties as well [22]. Thus, one can expect that such a diversity in the non-monophasic ReBCO ceramic's property might be useful for future practical application [22-24]. The presence of the magnetic Dy^{3+} cation in the crystal structure of the 123-phase and of the second magnetic phase of Fe_3O_4 provoked us to explore the effect of an external magnetic field on the superconducting transition temperature. Fig. 5 shows the resistivity as a function of the temperature without and with a magnetic field of 1 T. The onset of the resistivity drop is seen at 94 K ($T_{c-onset}$) in both cases, which is typical for intragrain superconductivity. The second maximum at 36 K and 12 K for measurements without and with external magnetic field, respectively, is due to the intragrain superconductivity. The $T_{c-onset}$ is higher compared with the value reported for pure polycrystalline DyBCO [12]. We presume that this is due to the presence of Fe_3O_4 nanoparticles and $BaCuO_2$ and CuO phases at the grain boundaries that improves the grain connectivity.

CONCLUSIONS

Using XRD analysis, the cell volume (*V*) of the superconducting phase (Dy123) of bulk samples was calculated.

Its values for a pure Dy123 and Dy123 with Fe_3O_4 additive were found to be the same. XRD analysis was conducted on the entire surface of the samples and did not detect phases whose amount was below 4%. EDX analysis was performed at a specific spot only and thus was able to detect other phases despite their small amounts. SEM micrographs revealed a multiphase structure with elongated grains for the DyBCO ceramic. Introducing Fe_3O_4 to the composition of the multiphasic DyBCO sample investigated did not interfere with the formation of the Dy123 superconducting phase, as well as with the formation of the $BaCuO_2$ and CuO phases. The EDX results and the mapping analyses pointed to the presence of small quantities of Fe on the surface scattered around the Dy123, CuO and $BaCuO_2$ crystals, which led us to the conclusion that Fe did not react with the other elements and did not form phases of its own, nor did it enter the lattice cells of the other phases. The calculated oxygen content in the samples did not vary significantly between the sample with Fe_3O_4 and the pure one. We, therefore, assumed that adding 2 wt.% of Fe_3O_4 nanopowder to the DyBCO ceramic did not influence the amount of oxygen, its value playing an important role in the material's superconducting properties.

REFERENCES

1. C. Andreouli, A. Tsetsekou, *Journal of the European Ceramic Society*, **20**(12), 2101 (2000).
2. A. Matsuda, K. Kinoshita, T. Ishii, H. Shibata, T. Watanabe, T. Yamada, *Physical Review B*, **38**(4), 2910 (1988).
3. P. Wei, H. W. Ying, Z. Q. Qi, *Physica C: Superconductivity*, **209**(4), 400 (1993).
4. H. C. Kao, F. C. Yu, W. Guan, *Physica C: Superconductivity*, **292**(1-2), 53 (1997).
5. P. Chainok, T. Khuntak, S. Sujinnapram, S. Tiyasri, W. Wongphakdee, T. Kruaehong, T. Nilkamjon, S. Ratreng, P. Udomsamuthirun, *International Journal of Modern Physics B*, **29**(09), 1550060 (2015).
6. W. Brenig, *Physics Reports*, **251**(3-4), 153 (1995).
7. E, Dagotto, *Reviews of Modern Physics,* **66**(3) 763 (1994).
8. M. Karppinen, H. Yamauchi, *International Journal of Inorganic Materials*, **2**(6), 589 (2000).
9. Q. X. Jia, B. Maiorov, H. Wang, Y. Lin, S. R. Foltyn, L. Civale, J. L. MacManus-Driscoll, *IEEE*

Transactions on Applied Superconductivity, **15**(2), 2723 (2005).

10. J. L. MacManus-Driscoll, S. R. Foltyn, Q. X. Jia, H. Wang, A. Serquis, B. Maiorov, L. Civale, Y. Lin, M. E. Hawley, M. P. Maley, D. E. Peterson, *Applied Physics Letters*, **84**(26), 5329 (2004).

11. H. Zhou, B. Maiorov, H. Wang, J. L. MacManus-Driscoll, T. G. Holesinger, L. Civale, Q. X. Jia, S. R. Foltyn, *Superconductor Science and Technology*, **21**(2), 025001 (2007).

12. T. Koutzarova, I. Nedkov, M. Ausloos, R. Cloots, T. Midlarz, M. Nogues, *Phys. Stat. Sol. (a)*, **191,** 235 (2002).

13. P. Boonsong, P. Wannasut, A. Rachakom, A. Watcharapasorn, *Chiang Mai Journal of Science*, **45**(4), 1835 (2018).

14. A. Veneva, I. Iordanov, L. Toshev, A. Stoyanova-Ivanova, D. Gogova, *Physica C: Superconductivity*, **308**(3-4), 175 (1998).

15. B. Khoshnevisan, M. Mohammadi, *Physica C: Superconductivity and Its Applications*, **523**, 5 (2016).

16. K. Tantivichitvech, S. Sirininlakul, W. Bunyoprakan, T. Nilkamjon, R. Supadanaison, S. Tiyasri, W. Wongphakdee, P. Udomsamuthirun, *Science and Technology RMUTT Journal*, **8** (2), 73 (2018).

17. S. N. Abd-Ghani, R. Abd-Shukor, W. Kong, *Advanced Materials Research,* **501**, 309 (2012), Trans Tech Publications Ltd.

18. W. Malaeb, H. Basma, R. Awad, T. Hibino, Y. Kamihara, *Journal of Superconductivity and Novel Magnetism*, **32**(10), 3065 (2019).

19. T. Koutzarova, S. Kolev, C. Ghelev, D. Paneva, I. Nedkov, *Physica Status Solidi C*, **3**(5), 1302 (2006).

20. P. Boonsong, P. Wannasut, S. Buntham, A. Rachakom, C. Sriprachuabwong, A. Tuantranont, A. Watcharapasorn, *Chiang Mai Journal of Science*, **45**(7), 2809 (2018).

21. A. Stoyanova-Ivanova, T. St. Georgieva, L. Dimova, B. Shivachev, *Bulgarian Chemical Communications*, **43**(2), 320 (2011).

22. A. K. Stoyanova-Ivanova, S. D. Terzieva, S. I. Georgieva, B. S. Blagoev, D. G. Kovacheva, A. Zaleski, V. Mikli, *Romanian Journal of Physics*, **63**(1-2), 1 (2018).

23. K. Sreedhar, P. Ganguly, *Inorganic Chemistry*, **27**(13), 2261 (1988).

24. P. Ganguly, K. Sreedhar, A. R. Raju, G. Demazeau, P. Hagenmuller, *Journal of Physics: Condensed Matter*, **1**(1), 213 (1989).

25. A. Thompson, D. Attwood, E. Gullikson, M. Howells, K. J. Kim, J. Kirz, J. Kortright, I. Lindau, P. Pianetta, A. Robinson, J. Scofield, X-ray Data Booklet, Lawrence Berkeley National Laboratory, University of California, Berkeley, CA, 94720, 2001.